



Ozone-assisted regeneration of magnetic carbon nanotubes for removing organic water pollutants



Mohamed Ateia^{a,*}, Marcel Ceccato^b, Akin Budi^b, Evren Ataman^b, Chihiro Yoshimura^a, Matthew S. Johnson^c

^a Department of Civil and Environmental Engineering, Tokyo Institute of Technology, 2-12-1-M1-4 Ookayama, Tokyo 152-8552, Japan

^b Nano-Science Center, Department of Chemistry, University of Copenhagen, Universitetsparken 5, DK-2100 Copenhagen, Denmark

^c Department of Chemistry, University of Copenhagen, Universitetsparken 5, DK-2100 Copenhagen, Denmark

GRAPHICAL ABSTRACT



ARTICLE INFO

Keywords:

Ozone
Ethanol
Regeneration
Magnetic carbon nanotubes
Degradation byproducts
Atrazine
XPS
DFT

ABSTRACT

There is a significant interest in sustainable and eco-friendly methods of regenerating spent nanomaterials in order to use resources more efficiently and minimize the cost of materials and techniques. This paper investigates the feasibility of using ozone to regenerate magnetic carbon nanotubes (MCNTs) after they have been used to remove organic pollutants from water. We ran MCNT through multiple regeneration cycles (i.e. magnetic collection → ozone regeneration → washing with ethanol then water) to adsorb atrazine. The results of our adsorption experiments show that the atrazine removal capacity of the MCNTs decreased from 57.8 to 27.6 mg/g in three cycles if only ozone treatment is used as a regeneration method. However, this capacity increased when MCNTs are washed with ethanol following ozone treatment. MCNTs were seen to retain 85–93% of its original adsorption affinity even after ten consecutive regeneration cycles. Additionally, we used a three layer graphite slab as a model system for CNTs and performed density functional theory (DFT) calculations to determine the free energy of adsorption and the free energy of solvation of atrazine and its byproducts in water and ethanol. The results of X-ray photoelectron spectroscopy (XPS) measurements and DFT calculations showed that $\pi-\pi$ interactions of MCNTs were not affected by ozonation and/or washing with ethanol and this procedure could remove the degradation byproducts attached on the surface. Overall, this is the first report that demonstrates the feasibility of regenerating spent MCNTs using ozone assisted by ethanol washing as an efficient and facile treatment.

* Corresponding author.

E-mail address: iateia@clemsun.edu (M. Ateia).

<http://dx.doi.org/10.1016/j.cej.2017.10.166>

Received 26 July 2017; Received in revised form 25 October 2017; Accepted 29 October 2017

Available online 31 October 2017

1385-8947/ © 2017 Elsevier B.V. All rights reserved.

1. Introduction

Pollution control using adsorption is a widely used technology that requires low energy and aims to confine diverse compounds using a variety of adsorbent materials. Carbon nanotubes (CNTs) have been extensively studied as adsorbents for a wide variety of organic pollutants (e.g., pesticides [1], pharmaceuticals [2], volatile organic compounds [3], dyes [4,5], phenols [6,7], and natural organic matter [8]) owing to their high surface area to mass ratio, porosity, and rapid sorption kinetics [9,10]. However, adsorption-based technologies are nondestructive and adsorbed pollutants are not degraded. Thus, regeneration and management of spent adsorbents are critical to the sustainability of adsorption-based systems. Recently, a number of regeneration techniques have been used to recycle CNTs and reduce the treatment cost. Examples include using microwaves [11], desorption solutions [12], ultrasound [13], and ozone [14]. Among these, ozone regeneration was found to be simple, scalable and cost-effective. The interaction between functional groups on CNTs and ozone generates hydroxyl radicals which further accelerate the degradation of pollutants during the regeneration process [15,16].

A major concern in using oxidation to regenerate carbonaceous materials is how changes in surface oxygen content would affect the removal capacity for organic pollutants by adsorption. In this regard, there are different reports in the literature based on the target pollutant. Sheng, et al. [17], Li, et al. [18], and Yu, et al. [19] reported that increasing oxygen content may increase the hydrophilicity and the surface negative charges of CNTs, and therefore reduce their adsorption capacity towards some hydrophobic organic pollutants. On the other hand, Yu, et al. [20] and Piao, et al. [21] suggested that elevating oxygen content and hydrophilicity would also disperse CNTs and increase their affinity towards organic chemicals with higher polarity and lower molecular weight. However, it's important to note that previous studies have used nitric acid as the oxidizing agent, which has subsequently been shown to destroy the graphitic structure of CNTs [22].

To date, only one study addressed using ozone to regenerate spent CNTs [14]. In that study, the authors concluded that the surface oxygen content of CNTs was increased and, as a result, the adsorption capacity decreased for the removal of organic pollutants and increased for the removal of dissolved metals. This interpretation raises some concerns. First, the authors derived the oxygen content based on changes in C 1s X-ray photoelectron spectra, while it would be more accurate to use also O 1s spectra and surface composition derived from the survey spectra, to obtain a more reliable assessment of the C 1s spectra. Second, the authors linked the reduction in adsorption capacity to a weakening of $\pi-\pi$ interactions without providing supporting evidence. Meanwhile, a previous study showed negligible decrease of the $\pi-\pi$ interactions after ozonation of CNTs [23]. Third, the reported enhancement of dissolved metal removal suggests that the adsorption sites were probably still occupied by residuals from the organic chemical or its degradation byproducts [24]. Therefore, there is still a need for comprehensive investigation to examine the regeneration of CNTs using ozone to remove organic pollutants.

The main objective of this study was to systematically investigate the regeneration potential of CNTs using ozone and to identify, for the first time, the primary reason for the drop of adsorption capacity for organic pollutants on CNTs after ozonation. We targeted the adsorption and degradation of atrazine, one of the most harmful and widely used s-triazine herbicides for the control of broad leaf and grassy weeds in agricultural fields, as a model organic pollutant in water environment. To the best of our knowledge, this is also the first study to employ detailed XPS analysis and DFT calculations to evaluate the performance of regenerating spent adsorbents.

2. Materials and methods

2.1. Materials

CNTs were purchased from Chengdu Alpha Nano Technology Co.,

Chinese Academy of Science, China (surface area, $\sim 96 \text{ m}^2/\text{g}$; diameter, 10–20 nm; porosity, $0.4 \text{ cm}^3/\text{g}$; length, $\sim 20 \mu\text{m}$; purity, $> 98\%$). The Brunauer–Emmett–Teller (BET) surface areas, pore volumes and pore size distributions were measured from nitrogen physisorption data at 77 K obtained with ASAP 2020 analyzer (Micromeritics Instrument Corp. U.S.).

Ethanol (Sigma-Aldrich Co., Denmark) was used to prepare the magnetic adsorbents. A stock solution of atrazine (500 mg/L) was prepared by dissolving 50 mg of standard atrazine powder (Sigma-Aldrich Co., Japan; purity, 99%) in 100 mL of LC/MS grade methanol (Sigma-Aldrich Co., Japan) and kept refrigerated ($4 \text{ }^\circ\text{C}$). Standard solutions were prepared by diluting the stock solution in appropriate amounts of ultrapure deionized water (Milli-Q; conductivity $< 0.1 \mu\text{S}/\text{cm}$).

Ozone was produced using pure gaseous oxygen with a laboratory scale ozone generator (model ACF-1000; Infuser, Denmark) at an average gas flow rate of 1 L/min. Total ozone concentration in water samples was $6 \pm 2.1 \text{ mg/L}$, as measured using spectrophotometric method using reagent test kit (Spectroquant® Merck, Millipore CO., USA).

2.2. Approach

We hypothesized that the surface adsorption sites of CNTs are blocked after ozonation by the degradation byproducts of the organic chemicals. We tested this hypothesis by combining both experimental and theoretical approaches. First, we used magnetic carbon nanotubes with good magnetic response and easy separation ability, and ran multiple consecutive regeneration cycles (i.e. adsorption \rightarrow collection \rightarrow ozone regeneration \rightarrow washing with ethanol then water) (detailed methods are described in Section 2.3). Then, we characterized the material at each step using XPS. Second, we used DFT to calculate the free energy of adsorption and the free energy of solvation of atrazine and its byproducts in both water and ethanol.

2.3. Preparation of magnetic carbon nanotubes

Magnetic carbon nanotubes (MCNTs) were prepared using a facile method as reported in our previous study [25]. We dispersed approximately 0.5 g of CNTs in 100 mL of ethanol with a sonicator. Next, a we placed a permanent magnet (Nd-Fe-B MAGNET, Magna Co., Japan) on the outside of the glass flask. This step was repeated 3–4 times to attract of the magnetic fraction and separate it from the non- and low-magnetic material. Next, we repeated the same procedure using water as a solvent. The result of this procedure was a material that quickly responded to the magnetic separation procedure. Finally, we washed the collected MCNTs with water 3–4 times, dried, and stored them prior to use.

2.4. Adsorption experiments

Adsorption experiments were performed in 100 mL glass bottles using a regulated speed shaker at 100 rpm in a controlled temperature environment ($25 \pm 2 \text{ }^\circ\text{C}$). The adsorption process was studied as a function of initial atrazine concentration (1–30 mg/L) and MCNT concentration of 500 mg/L with a contact time of 180 min [25]. After the adsorption, the samples were filtered through a membrane filter ($0.45 \mu\text{m}$ PES filter, Membrane Solutions, Japan), and analyzed for atrazine concentrations. Blank experiments (with no adsorbents) were conducted in parallel, and the change in atrazine concentrations in blanks were found negligible.

The concentrations of atrazine were determined using high performance liquid chromatography (HPLC; SHIMADZU Prominence UFLC, Japan) equipped with a pump (Shimadzu, model: LC-20AD) and an UV-Vis absorbance detector (SPD-20A UFLC), with a C18 Column, Kinetex $5 \mu\text{m}$, $4.6 \times 250 \text{ mm}$ (Phenomenex CO., USA) operated with UV-Vis detection at 222 nm, a methanol–water (60: 40, v/v) mobile phase, a

100 μL injection volume, a 1 mL/min flow rate and 10 $\mu\text{g/L}$ minimum detection limit (MDL). All experiments were run in triplicate and the results are presented as the mean \pm standard error.

2.5. Ozone regeneration experiments

To examine the effect of degradation byproducts on the MCNTs, two different regeneration scenarios were tested (Fig. S1). In the first scenario, the spent MCNTs after adsorption were ozonated in pure water at room temperature in a flask with an ozone inlet pipe that reaches the bottom of the flask. Then, the ozonated MCNTs were collected using a magnet, the supernatant was removed, and the collected MCNTs were washed with water and reused for adsorption. In the second scenario, the spent MCNTs were ozone-treated as described above, collected with magnet, washed with ethanol, washed with water, and then reused for adsorption. Further, the effect of the selected treatments on the raw MCNTs was tested independently and no changes on the material properties were seen. The weight of the adsorbents was recorded before and after the experiments and the weight-loss of MCNTs was negligible. All experiments were run at two different ozone exposure times, 20 min and 60 min.

2.6. Spectroscopy measurements

The surface characteristics of MCNTs at different steps of the process (i.e. before and after adsorption and ozonation) were examined using Fourier transform infrared spectroscopy (FT-IR) and XPS. XPS analysis was performed with a Kratos Axis Ultra^{DLD} instrument operated with a monochromatic $\text{AlK}\alpha$ X-ray source ($h\nu = 1486.6$ eV) at a power of 150 W. Survey scans were acquired in the 0–1350 eV range at a pass energy of 160 eV and step size of 0.5 eV. High-resolution scans of C 1s (276–310 eV), O 1s (524–550 eV), and N 1s (387–412 eV) regions were acquired at a pass energy of 10 eV and step size of 0.1 eV. The generated XPS data were processed using the CasaXPS software. Atomic surface concentrations were determined by fitting the core level spectra using Gaussian-Lorentzian line shapes and a Shirley background; the value reported represents the average of at least two measurements. Only minor variations in surface composition were observed between the first and last spectra collected, indicating that surface damage induced by the X-ray exposure is negligible. The systematic error is estimated to be in the order of 5–10% and the measurements were done using a spot size of 0.21 mm^2 . A JEOL JIR-SPX200 Japan was used to determine the FTIR spectra in the wavenumber range of 250 cm^{-1} to 4200 cm^{-1} . X-ray diffraction (XRD) diffractograms were acquired with Cu $\text{K}\alpha_{1,2}$ (1.5406 Å), Ni-filtered radiation on a Bruker D8 Advance instrument equipped with a LynxEye PSD detector. Diffractograms were collected in the range of 15–70° 2 θ with 0.03° 2 θ step size and 8 s time step, while the sample was spun at 15 rpm. The divergence slit was set to 0.3°, antiscatter slit to 3°, primary and secondary Soller slits were 2.5° and the detector window opening was 2.71°.

2.7. Density functional theory calculations

We used the all-electron atomic orbital based DFT code, DMol³, in this work [26,27]. The Perdew, Burke, and Erzenhof (PBE) exchange-correlational functional [28] was used, within the generalized gradient approximation [29]. The basis set used was a double numerical type with polarization. The Grimme dispersion correction was used to account for weak dispersion interactions [30]. All of the calculations were performed at the Gamma point. The electronic convergence criterion was 2.7×10^{-4} eV, and the geometries converged to 10^{-4} Å with the forces converged to 2.7×10^{-2} eV/Å.

The atrazine molecule and its ozonation byproducts were obtained from Adams and Randtke [31]. In particular, we focused on CIAT, C-AAT, CDAT, OEAT, and OIAT, as well as the intact atrazine (CIET). Fig. S2 shows the suggested degradation pathway. For computational

simplicity, graphite was used to model CNTs. To create the graphite slab, we first created and geometry optimized bulk graphite to ensure there were no residual stresses in the superstructure. A 3-layer $[5 \times 5]$ supercell was then created, yielding a hexagonal cell with side length of 12.3 Å. In all the simulations, the middle layer of graphite was kept fixed while the rest of the graphite layers and molecule of interest were allowed to move. Fig. 1 shows the optimized structure of target molecules in this study on graphite.

COSMO-RS [32,33] with DMOL3_PBE_C30_1301 parameter set was used to obtain the free energy of solvation (G_{solv}) in different solvents. The Gibbs free energy of the reaction thus becomes:

$$\Delta G = \Delta H + \Delta G_{\text{solv}} \quad (1)$$

where ΔG is the free energy of adsorption, ΔH is the change in enthalpy in vacuum, and ΔG_{solv} is the change in free energy of solvation.

3. Results and discussion

3.1. Adsorption–regeneration experiments

The results of adsorption isotherms and the corresponding Langmuir isotherm model (Eq. (2)) for the initial condition and the regeneration experiments are presented in Table 1. Table 2

$$Q_e = \frac{Q_{\text{Max}} b C_e}{1 + b C_e} \quad (2)$$

where Q_e (mg/g) is the adsorption capacity, C_e (mg/L) is the equilibrium concentration, Q_{max} (mg/g) is the maximum capacity of adsorbate required to form a complete monolayer on the surface, and b is the Langmuir constant.

The Langmuir isotherm model showed good fit with the experimental data as indicated by the coefficient of determinations (R^2) of 0.98–0.99 (Table 1) and was used to describe the adsorption of atrazine on MCNTs. This agrees with previous reports of atrazine adsorption on single-walled CNTs [34] and multi-walled CNTs [35]. Fig. 2A shows that the adsorption capacity was highest for raw MCNTs at 57.8 mg/g and dropped to 44.5, 37.5, and 27.6 mg/g after the first, second, and third ozone regeneration cycle, respectively. By extending the experiment to ten regeneration cycles, the removal was as low as 30–35% of the initial removal capacity (Fig. 3). On the other hand, Fig. 2B shows that washing the ozone treated MCNTs in ethanol could recover the adsorption capacity of the MCNTs. After ten regeneration cycles, the performance was stable and ranged between 85 and 93% of the initial removal capacity (Fig. 3). We interpret this result as an indication that the ozonation byproducts occupy adsorption sites after ozonation, and that ozone itself had minimal effect on the surface characteristics of MCNT. These observations were further confirmed by checking the surface composition of MCNTs as explained in the following section.

3.2. Material characterization

Before adsorption. The previous report by Wang, et al. [14] claimed that the removal capacity reduction for organic compounds occurred solely due to weakened π – π interactions after the introduction of oxygen-containing functional groups to the surface of MCNTs. However, we tested the effect of ozone on the characteristics of MCNTs prior to adsorption experiments and we observed no significant change in surface oxygen content or π – π interactions as measured by XPS (samples C1 and C2 in Table 3). Further, the magnetic particles were located in the interior of the tubes and protected by layers of graphene sheets (Fig. S3A). Therefore, they are sequestered from oxidation during the ozonation process. Samples collected before and after ozone pre-treatment showed two dominant XRD diffraction peaks at 42°, 44°, and 52° 2 θ that were assigned to graphite-like structure and Ni (Fig. S3B) [36]. In addition, FTIR spectra showed similar features, with four main broad bands at around 3420, 2925, 1645, and 1380 cm^{-1} , which

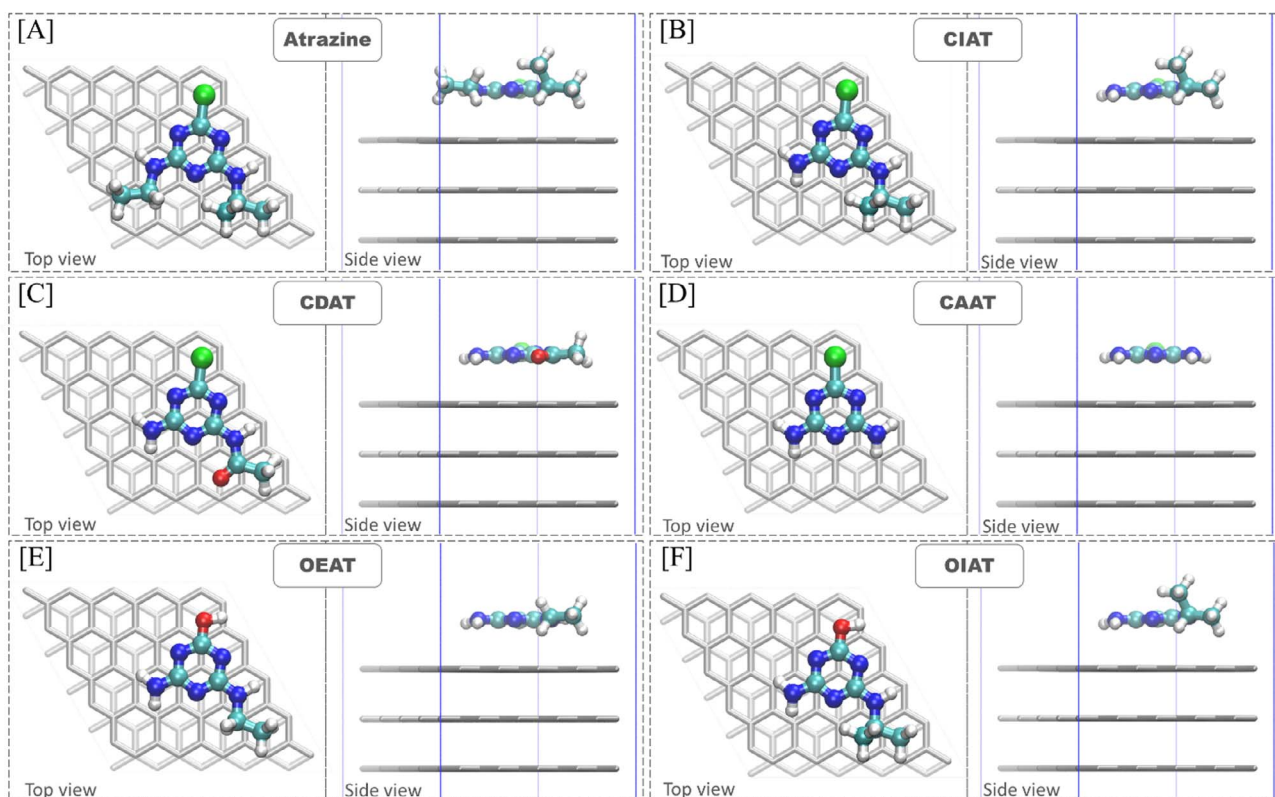


Fig. 1. Top and side views of the optimized structure of [A] atrazine and its ozonation byproducts ([B] CIAT, [C] CDAT, [D] CAAT, [E] OEAT, [F] OIAT) on graphite. Carbon is shown in cyan, nitrogen in blue, chlorine in green, hydrogen in white, and graphite in gray.

were ascribed to the stretching vibrations of O–H, C–H, C=C, and C–H bonds, respectively (Fig. S3C) [37–39]. These results suggest that ozone treatment scarcely changed the surface functional groups of the MCNTs. This is in agreement with previous observations by Morales-Lara, et al. [23].

After adsorption and ozone regeneration. We performed detailed analysis of the surface characteristics of MCNTs using XPS as shown in Fig. 4 and Fig. S4–S5 in SI. To evaluate the level of sp^2 hybridization of the samples, we estimated the D parameters [40] of the MWCNTs as received. We determined a D value of 22.5 corresponding to 100% sp^2 hybridization [41]. The C 1s spectra were fitted with an asymmetric peak at 284.4 eV corresponding to the sp^2 graphitic structure [42] and two peaks at 286.3 eV and 288.1 eV are assigned to C–O and C=O groups. Further, two $\pi-\pi^*$ type shake-up peaks were identified at 6.7 eV and 9.8 eV, higher binding energies, from the main peak [43]. The C 1s spectrum of atrazine powder presented three peaks at 285.0, 286.2, and 288.1 eV, which were assigned to C–C and C–H bonds, C–N/C–O single bonds, and the atrazine ring function N–C=N, respectively (Table 3) [44]. The presence of atrazine or its byproducts after the adsorption process was detected by tracking nitrogen and/or chlorine on the surface of MCNTs. After adsorption of atrazine on MCNTs, the

Table 1
Parameters for the Langmuir isotherm for atrazine adsorption.

Regeneration method		Q_{Max} (mg/g) ^a	b (L/mg) ^a	R^2
Pristine MCNTs		57.8 [± 3.2]	0.28 [± 0.11]	0.98
Only ozone	Cycle 1	44.5 [± 1.6]	0.28 [± 0.17]	0.98
	Cycle 2	37.5 [± 2.1]	0.22 [± 0.12]	0.99
	Cycle 3	27.6 [± 1.2]	0.18 [± 0.11]	0.99
Ozone → washing with ethanol → washing with H ₂ O	Cycle 1	53.4 [± 2.4]	0.22 [± 0.06]	0.98
	Cycle 2	55.2 [± 1.3]	0.19 [± 0.16]	0.99
	Cycle 3	52.1 [± 4.1]	0.24 [± 0.09]	0.99

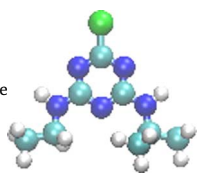
peaks at 286.3 eV and 288.1 eV increase, very likely due to the C–N and C–N=C groups present in the atrazine molecules (sample C3 in Table 3). The ratio between the peaks was 3.1:2.3:2.9, which is in good agreement with the expected theoretical value for atrazine of 3:2:3.

Tracking the nitrogen and/or chlorine at each step of the regeneration process revealed the presence of the degradation byproducts of atrazine after ozonating MCNT samples (samples C4 and C8 in Table 3). N 1s spectra of samples after adsorption of atrazine and ozone treatment were fitted with one component peak centered at 399.2–399.5 eV. This component was assigned to N in the atrazine ring (–N=) and in the –N– groups after adsorption of atrazine (Fig. S6) and also to acetamido (–NH–C=O) and imine/amine (–N=, –N) groups after the ozone treatment for 60 min. However, nitrogen and/or chlorine were not detected after washing the samples with ethanol. These results suggest that degradation byproducts remain attached after ozonation which confirms the adsorption results reported in the previous section. These findings were further confirmed by characterizing MCNT samples after 10 consecutive regeneration cycles (samples C7 and C11 in Table 3). In addition, we tested the effect of ozonation time by performing the regeneration experiments at 20 and 60 min. With 20 min ozonation time, the surface oxygen content in the first cycle slightly increased from 0.9% to 1.6% (samples C4–C6 in Table 3). Extending the ozonation time to 60 min, however, increased surface oxygen content by up to 4.9% (samples C8–C10 in Table 3). Despite this increase in the O content compared to C1 (blank sample), we observe only a 1% decrease of the $\pi-\pi^*$ type shake-up. For sample C2, after 20 min of ozone treatment, $\pi-\pi^*$ type shake-up, O and C concentrations are similar to sample C1. These results suggest that the oxygen-containing groups are formed mainly in already existing defects and the alteration of the graphitic structure is marginal, as observed previously by Morales-Lara et al. [23].

Increasing oxygen content may increase the hydrophilicity and reduce their adsorption capacity towards some organic pollutants or it might disperse CNTs and increase their adsorption affinity. FTIR spectra

Table 2
Chemical composition of atrazine powder derived from XPS.

Sample	Atom%					High Resolution C 1s		
	O	C	N	Cl	Na	C–C/C–H	C–N/C–O	N–C=N/C=O
Atrazine	1.1 [0.3]	59.6 [4.1]	31.5 [1.9]	7.5 [2.1]	0.3 [0.1]	37.2 [1.5]	27.6 [2.0]	35.3 [1.4]



Uncertainties from average values are shown in square brackets. Carbon is shown in cyan, nitrogen in blue, chlorine in green, and hydrogen in white.

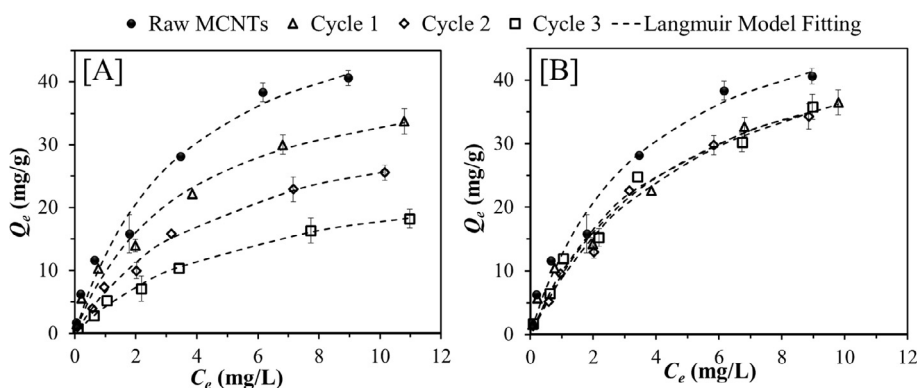


Fig. 2. Adsorption isotherms of atrazine on MCNTs and regeneration experiments using [A] only ozone treatment and [B] ozone treatment followed by desorption in ethanol. Experimental conditions: initial atrazine concentrations were 1–30 mg/L, $C_{MCNT} = 500$ mg/L, pH 7, $t = 180$ min, and $T = 25 \pm 2$ °C.

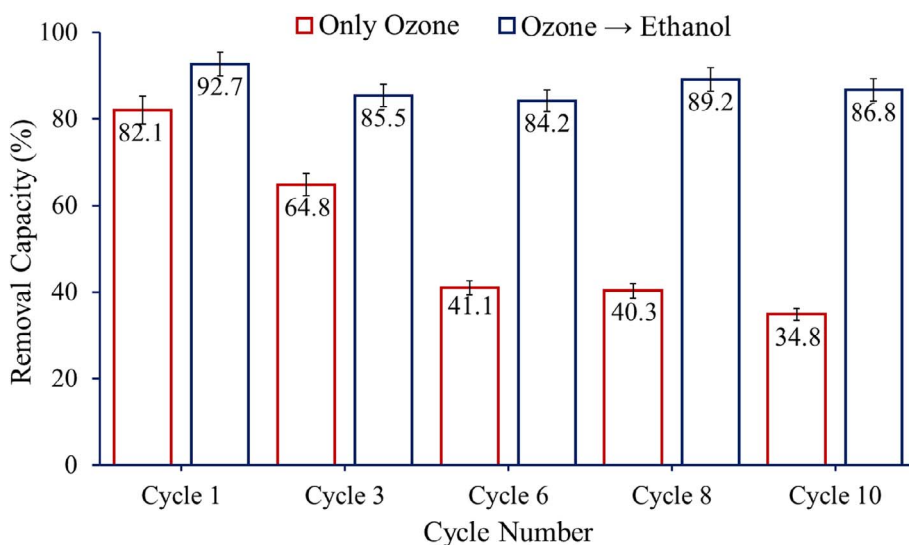


Fig. 3. Adsorption capacity and recovery rate for 10 consecutive regeneration cycles. Initial atrazine concentration was 5 mg/L and MCNT concentration was 500 mg/L at pH 7 ± 0.2 and the equilibrium time at 180 min.

show a slight increase in the signal for O–H and C=C bonds (Fig. 5). These observations are in line with XPS analysis. Apparently, the reduction of adsorption capacity of atrazine after ozonation followed by ethanol washing resulted from the introduction of oxygen-containing functional groups (e.g. hydroxyl) (Fig. 2B). Thus, we interpret the continuous reduction in the adsorption capacity after only ozonation (Fig. 2A) as re-adsorption of ozonation byproducts of atrazine (i.e., ozone itself had minimal effect on the surface characteristics of MCNT). These results enable the application of ozone regeneration of CNTs for organic degradation applications. More details about the binding between atrazine and selected major byproducts are discussed in the following section.

3.3. DFT calculation

Table 4 shows how the free energy of adsorption for atrazine and its ozonation breakdown products is affected by its environment. CIET was the strongest adsorbed molecule on graphite in all the environments considered in this study. The order of adsorption strength was found to be: vacuum > water > ethanol, which is observed in all the molecules. In all cases, the byproducts are more weakly adsorbed by an average of ~ 0.2 eV compared to intact atrazine (CIET), except for CAAT which is weaker by ~ 0.4 eV. This indicates that breaking down atrazine can help lower the energy barrier necessary to remove the organic pollutant from CNTs. Ethanol was selected based on its ability

Table 3
XPS derived chemical composition of the top ~10 nm of the MCNT surface (atom%).

Code	Sample	Atom%				High resolution C 1s			
		O	C	N	Cl	C=C	C–O	C=O	π - π^*
C1	Raw MCNT	1.1 [0.1]	98.9 [0.1]	N.D.	N.D.	82.7 [0.1]	0.5 [0.2]	0.7 [0.1]	16.1 [0.1]
C2	MCNT \rightarrow O ₃ (20 min)	0.9 [0.1]	99.1 [0.1]	N.D.	N.D.	83.1 [0.0]	0.3 [0.0]	0.7 [0.0]	15.9 [0.0]
C3	MCNT \rightarrow ATZ	0.8 [0.1]	97.7 [0.3]	1.1 [0.2]	0.38 [0.04]	84.0 [0.0]	0.9 [0.1]	1.3 [0.2]	13.8 [0.3]
C4	MCNT \rightarrow ATZ \rightarrow O ₃ (20 min)	0.9 [0.2]	97.9 [0.4]	0.9 [0.4]	0.3 [0.1]	83.3 [0.2]	0.9 [0.2]	1.1 [0.4]	14.7 [0.3]
C5	MCNT \rightarrow ATZ \rightarrow O ₃ (20 min) \rightarrow Ethanol	1.6 [0.0]	98.1 [0.01]	N.D.	0.07 [0.03]	82.0 [0.1]	0.8 [0.1]	2.0 [0.1]	15.2 [0.2]
C6	MCNT \rightarrow ATZ \rightarrow O ₃ (20 min) \rightarrow Ethanol \rightarrow H ₂ O	0.7 [0.1]	99.3 [0.1]	Traces (< 0.1)	N.D.	84.1 [0.1]	N.D.	0.7 [0.04]	15.2 [0.1]
C7	MCNT _{REC} \rightarrow ATZ \rightarrow O ₃ (20 min) \rightarrow Ethanol \rightarrow H ₂ O	3.1 [0.1]	95.6 [0.1]	0.14 [0.05]	0.20 [0.01]	81.8 [0.3]	0.4 [0.1]	1.4 [0.1]	15.1 [0.4]
C8	MCNT \rightarrow ATZ \rightarrow O ₃ (60 min)	4.9 [0.4]	91.9 [0.6]	0.1 [0.01]	0.3 [0.04]	82.4 [0.6]	1.0 [0.5]	1.7 [0.1]	14.8 [1.0]
C9	MCNT \rightarrow ATZ \rightarrow O ₃ (60 min) \rightarrow Ethanol	2.5 [0.1]	97.5 [0.1]	N.D.	N.D.	83.1 [0.4]	1.2 [0.1]	2.3 [0.1]	13.4 [0.3]
C10	MCNT \rightarrow ATZ \rightarrow O ₃ (60 min) \rightarrow Ethanol \rightarrow H ₂ O	2.2 [0.1]	97.4 [0.1]	N.D.	0.09 [0.0]	82.2 [1.1]	1.0 [0.1]	2.3 [0.2]	14.5 [1.2]
C11	MCNT _{REC} \rightarrow ATZ \rightarrow O ₃ (60 min) \rightarrow Ethanol \rightarrow H ₂ O	3.42 [0.01]	95.50 [0.01]	0.18 [0.01]	0.11 [0.02]	83.1 [0.5]	1.6 [0.2]	1.6 [0.1]	14.9 [0.4]

ATZ refers to atrazine. MCNT and MCNT_{REC} refer to magnetic carbon nanotubes before adsorption and after 10 regeneration cycles, respectively. Uncertainties from average values are shown in square brackets. N.D. refers to not detected.

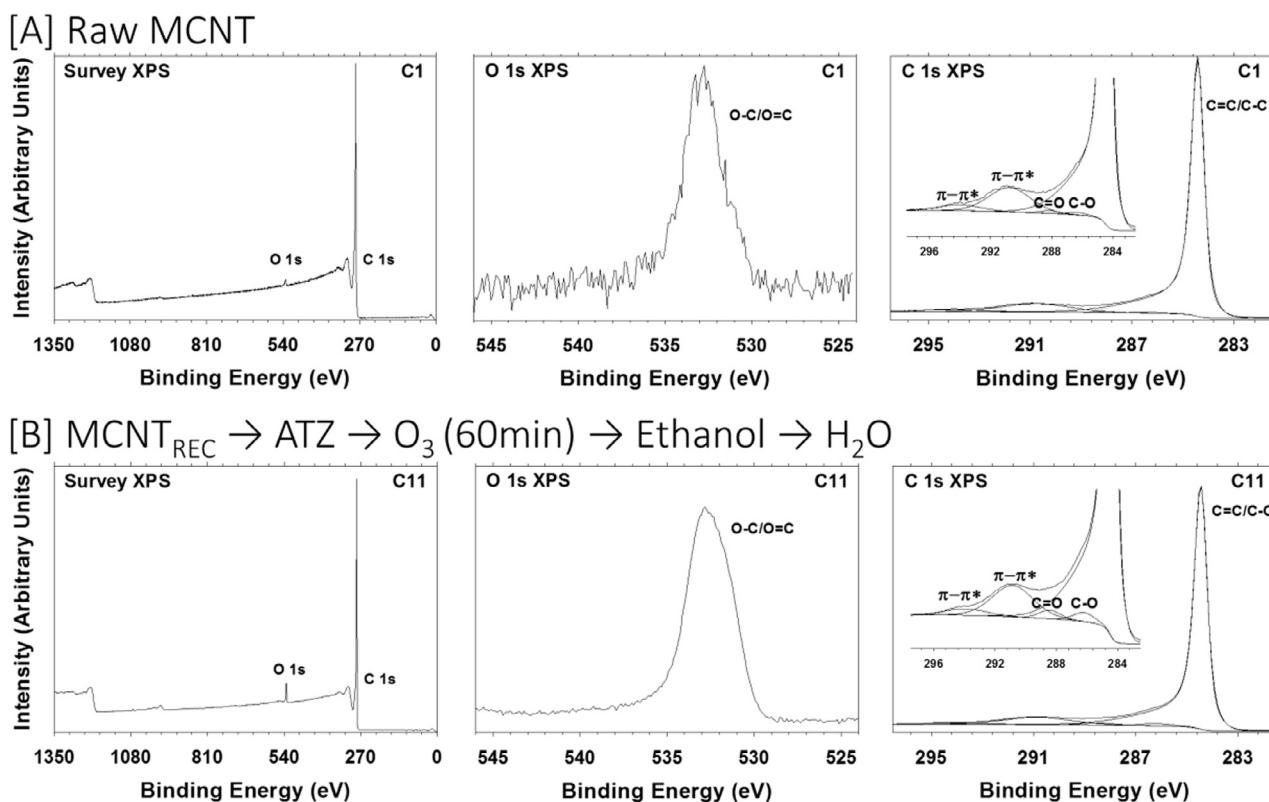


Fig. 4. The XPS full spectra, C 1s, and O 1s for samples [A] C1 in Table 3: Raw MCNT and [B] C11 in Table 3: MCNT_{REC} \rightarrow ATZ \rightarrow O₃ (60 min) \rightarrow Ethanol \rightarrow H₂O.

to solvate and suspend the CNTs and its viscosity, which maximized the separation efficiency and minimized the possibility of forming CNT bundles. The DFT calculation confirms that ethanol is a better solvent than water for removing oxidation byproducts from the surface of CNTs. In addition, one major advantage of using ethanol is its low boiling point. Therefore, distillation of ethanol can be an easy and ecofriendly recovery method.

It must be noted that we have only considered the free energy of adsorption of the individual molecules. Kinetic and reaction barriers are currently beyond the scope of this study. Therefore, from a purely energetics perspective, CAAT is the easiest form for removal from a graphitic structure. Adams and Randtke [31] identified CIAT, CAAT and CDAT as major breakdown products of atrazine, while OEAT and OIAT were identified as minor breakdown products and were only observed at conditions favoring hydroxyl radical production (Fig. S2). The production of OEAT and OIAT under ozonation is correlated with the

increase in the O XPS signal in sample C8 compared to sample C4 in Table 3.

4. Conclusions

In this study, we demonstrated the use of ozone to degrade adsorbed atrazine on the surface of MCNTs followed by washing with ethanol to remove adsorbed degradation byproducts. Detailed XPS analysis showed that ozonation does not affect the π - π interactions of MCNTs but results in the accumulation of atrazine dissociation products on the surface. The results of adsorption energy calculations indicate that it is possible to remove the degradation byproducts of atrazine simply by washing the MCNTs with ethanol. Our proposed approach is facile and efficient in using ozone to degrade the organic pollutants and to regenerate the spent MCNTs. The need for sustainable technologies and materials is more essential than ever in order to overcome

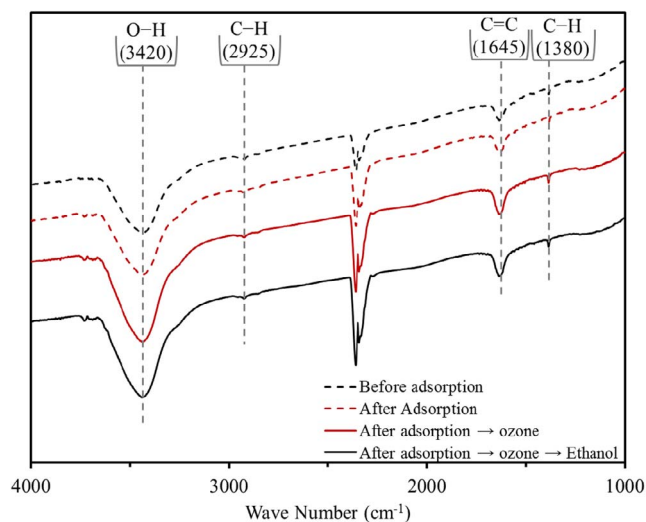


Fig. 5. FTIR spectra for samples at different steps in the experiments.

Table 4

Free energy of adsorption for atrazine and its breakdown products on graphite after ozonation.

Molecule	ΔH [eV]	ΔG [eV]	
		In water	In ethanol
CIET (Atrazine)	−1.25	−1.19	−0.94
CIAT	−1.05	−0.94	−0.75
CDAT	−1.05	−0.96	−0.78
CAAT	−0.83	−0.68	−0.53
OEAT	−1.02	−0.89	−0.74
OIAT	−1.02	−0.95	−0.79

Carbon is shown in cyan, nitrogen in blue, chlorine in green, oxygen in red, and hydrogen in white.

environmental, economic, and resource availability issues. Thus, more studies on the effect of water chemistry on the regeneration performance are recommended.

Acknowledgments

This work was supported in part by the Program for Leading Graduate School “Academy for Co-creative Education of Environment and Energy Science”, MEXT, Tokyo Institute of Technology and the JSPS Core-to-Core Program. We would like to thank the Infuser company of Denmark for providing the ozone generator. We thank Jonathan Quinson, Department of Chemistry, University of Copenhagen for providing the TEM image.

Appendix A. Supplementary data

Supplementary data associated with this article can be found, in the online version, at <http://dx.doi.org/10.1016/j.cej.2017.10.166>.

References

- [1] J.-G. Yu, X.-H. Zhao, H. Yang, X.-H. Chen, Q. Yang, L.-Y. Yu, J.-H. Jiang, X.-Q. Chen, Aqueous adsorption and removal of organic contaminants by carbon nanotubes, *Sci. Total Environ.* 482 (2014) 241–251.
- [2] C. Jung, A. Son, N. Her, K.-D. Zoh, J. Cho, Y. Yoon, Removal of endocrine disrupting compounds, pharmaceuticals, and personal care products in water using carbon nanotubes: a review, *J. Ind. Eng. Chem.* (2015).
- [3] J. Zheng, Q. Zhang, X. He, M. Gao, X. Ma, G. Li, Nanocomposites of carbon nanotube (CNTs)/CuO with high sensitivity to organic volatiles at room temperature, *Procedia Eng.* 36 (2012) 235–245.
- [4] F. Geyikçi, Adsorption of acid blue 161 (AB 161) dye from water by multi-walled carbon nanotubes, *Fullerenes Nanotubes Carbon Nanostruct.* 21 (2013) 579–593.
- [5] N. Tabrizi, M. Yavari, Methylene blue removal by carbon nanotube-based aerogels, *Chem. Eng. Res. Des.* (2014).
- [6] J. Xu, T. Sheng, Y. Hu, S.A. Baig, X. Lv, X. Xu, Adsorption–dechlorination of 2, 4-dichlorophenol using two specified MWCNTs-stabilized Pd/Fe nanocomposites, *Chem. Eng. J.* 219 (2013) 162–173.
- [7] O. Moradi, M. Yari, P. Moaveni, M. Norouzi, Removal of p-nitrophenol and naphthalene from petrochemical wastewater using SWCNTs and SWCNT-COOH surfaces, *Fullerenes Nanotubes Carbon Nanostruct.* 20 (2012) 85–98.
- [8] M. Ateia, O.G. Apul, Y. Shimizu, A. Muflihah, C. Yoshimura, T. Karanfil, Elucidating adsorptive fractions of natural organic matter on carbon nanotubes, *Environ. Sci. Technol.* (2017).
- [9] C. Santhosh, V. Velmurugan, G. Jacob, S.K. Jeong, A.N. Grace, A. Bhatnagar, Role of nanomaterials in water treatment applications: a review, *Chem. Eng. J.* 306 (2016) 1116–1137.
- [10] M. Ahmadi, H. Elmogny, T. Madrakian, M. Abdel-Rehim, Nanomaterials as sorbents for sample preparation in bioanalysis: a review, *Anal. Chim. Acta* 958 (2016) 1–21.
- [11] C. Cui, Q. Zheng, Y. Han, Y. Xin, Rapid microwave-assisted regeneration of magnetic carbon nanotubes loaded with p-nitrophenol, *Appl. Surf. Sci.* 346 (2015) 99–106.
- [12] Q. Song, H. Wang, B. Yang, F. Wang, X. Sun, A novel adsorbent of Ag-FMWCNTs for the removal of SMX from aqueous solution, *RSC Adv.* 6 (2016) 75855–75861.
- [13] E. Derakhshani, A. Naghizadeh, Ultrasound regeneration of multi wall carbon nanotubes saturated by humic acid, *Desalin. Water Treat.* 52 (2014) 7468–7472.
- [14] X. Wang, C. Chen, J. Li, X. Wang, Ozone degradation of 1-naphthol on multiwalled carbon nanotubes/iron oxides and recycling of the adsorbent, *Chem. Eng. J.* 262 (2015) 1303–1310.
- [15] A.G. Gonçalves, J.L. Figueiredo, J.J. Órfão, M.F. Pereira, Influence of the surface chemistry of multi-walled carbon nanotubes on their activity as ozonation catalysts, *Carbon* 48 (2010) 4369–4381.
- [16] R. Oulton, J.P. Haase, S. Kaalberg, C.T. Redmond, M.J. Nalbandian, D.M. Cwiertyny, hydroxyl radical formation during ozonation of multiwalled carbon nanotubes: performance optimization and demonstration of a reactive CNT filter, *Environ. Sci. Technol.* 49 (2015) 3687–3697.
- [17] G. Sheng, D. Shao, X. Ren, X. Wang, J. Li, Y. Chen, X. Wang, Kinetics and thermodynamics of adsorption of ionizable aromatic compounds from aqueous solutions by as-prepared and oxidized multiwalled carbon nanotubes, *J. Hazard. Mater.* 178 (2010) 505–516.
- [18] X. Li, H. Zhao, X. Quan, S. Chen, Y. Zhang, H. Yu, Adsorption of ionizable organic contaminants on multi-walled carbon nanotubes with different oxygen contents, *J. Hazard. Mater.* 186 (2011) 407–415.
- [19] X. Yu, L. Zhang, M. Liang, W. Sun, pH-dependent sulfonamides adsorption by carbon nanotubes with different surface oxygen contents, *Chem. Eng. J.* 279 (2015) 363–371.
- [20] F. Yu, Y. Wu, J. Ma, Influence of the pore structure and surface chemistry on adsorption of ethylbenzene and xylene isomers by KOH-activated multi-walled carbon nanotubes, *J. Hazard. Mater.* 237 (2012) 102–109.
- [21] L. Piao, Q. Liu, Y. Li, C. Wang, Adsorption of L-phenylalanine on single-walled

- carbon nanotubes, *J. Phys. Chem. C* 112 (2008) 2857–2863.
- [22] J. Vejpravova, B. Pacakova, M. Kalbac, Magnetic impurities in single-walled carbon nanotubes and graphene: a review, *Analyst* 141 (2016) 2639–2656.
- [23] F. Morales-Lara, M.J. Pérez-Mendoza, D. Altmajer-Vaz, M. García-Román, M. Melguizo, F.J. López-Garzón, M. Domingo-García, Functionalization of multi-wall carbon nanotubes by ozone at basic pH comparison with oxygen plasma and ozone in gas phase, *J. Phys. Chem. C* 117 (2013) 11647–11655.
- [24] D. Shao, X. Ren, J. Hu, Y. Chen, X. Wang, Preconcentration of Pb 2+ from aqueous solution using poly (acrylamide) and poly (N, N-dimethylacrylamide) grafted multiwalled carbon nanotubes, *Colloids Surf. A* 360 (2010) 74–84.
- [25] M. Ateia, C.B. Koch, S. Jelavic, A.M. Hirt, J. Quinson, C. Yoshimura, M.S. Johnson, Green and facile approach for enhancing the inherent magnetic properties of carbon nanotubes for water treatment application, *PLOS ONE* (2017).
- [26] B. Delley, An all-electron numerical method for solving the local density functional for polyatomic molecules, *J. Chem. Phys.* 92 (1990) 508–517.
- [27] B. Delley, From molecules to solids with the DMol 3 approach, *J. Chem. Phys.* 113 (2000) 7756–7764.
- [28] J.P. Perdew, K. Burke, M. Ernzerhof, Generalized gradient approximation made simple, *Phys. Rev. Lett.* 77 (1996) 3865.
- [29] J.P. Perdew, J.A. Chevary, S.H. Vosko, K.A. Jackson, M.R. Pederson, D.J. Singh, C. Fiolhais, Atoms, molecules, solids, and surfaces: applications of the generalized gradient approximation for exchange and correlation, *Phys. Rev. B* 46 (1992) 6671.
- [30] S. Grimme, Semiempirical GGA-type density functional constructed with a long-range dispersion correction, *J. Comput. Chem.* 27 (2006) 1787–1799.
- [31] C.D. Adams, S.J. Randtke, Ozonation byproducts of atrazine in synthetic and natural waters, *Environ. Sci. Technol.* 26 (1992) 2218–2227.
- [32] A. Klamt, Conductor-like screening model for real solvents: a new approach to the quantitative calculation of solvation phenomena, *J. Phys. Chem.* 99 (1995) 2224–2235.
- [33] A. Klamt, V. Jonas, T. Bürger, J.C. Lohrenz, Refinement and parametrization of COSMO-RS, *J. Phys. Chem. A* 102 (1998) 5074–5085.
- [34] X. Yan, B. Shi, J. Lu, C. Feng, D. Wang, H. Tang, Adsorption and desorption of atrazine on carbon nanotubes, *J. Colloid Interface Sci.* 321 (2008) 30–38.
- [35] W.-W. Tang, G.-M. Zeng, J.-L. Gong, Y. Liu, X.-Y. Wang, Y.-Y. Liu, Z.-F. Liu, L. Chen, X.-R. Zhang, D.-Z. Tu, Simultaneous adsorption of atrazine and Cu (II) from wastewater by magnetic multi-walled carbon nanotube, *Chem. Eng. J.* 211 (2012) 470–478.
- [36] S. Al Khabouri, S. Al Harthi, T. Maekawa, Y. Nagaoka, M.E. Elzain, A. Al Hinai, A. Al-Rawas, A. Gismelseed, A.A. Yousif, Composition, electronic and magnetic investigation of the encapsulated ZnFe₂O₄ nanoparticles in multiwall carbon nanotubes containing Ni residuals, *Nanoscale Res. Lett.* 10 (2015) 1–10.
- [37] X. Fu, H. Yang, K. He, Y. Zhang, J. Wu, Enhanced photocatalytic activity of nano titanium dioxide coated on ethanol-soluble carbon nanotubes, *Mater. Res. Bull.* 48 (2013) 487–494.
- [38] J. Zou, X. Zhang, J. Zhao, C. Lei, Y. Zhao, Y. Zhu, Q. Li, Strengthening and toughening effects by strapping carbon nanotube cross-links with polymer molecules, *Compos. Sci. Technol.* 135 (2016) 123–127.
- [39] H. Kim, K.H. Ahn, S.J. Lee, Conductive poly (high internal phase emulsion) foams incorporated with polydopamine-coated carbon nanotubes, *Polymer* (2017).
- [40] Y. Mizokawa, T. Miyasato, S. Nakamura, K.M. Geib, C.W. Wilmsen, Comparison of the CKLL first-derivative auger spectra from XPS and AES using diamond, graphite SiC diamond-like-carbon films, *Surf. Sci.* 182 (1987) 431–438.
- [41] J. Lascovich, R. Giorgi, S. Scaglione, Evaluation of the sp²/sp³ ratio in amorphous carbon structure by XPS and XAES, *Appl. Surf. Sci.* 47 (1991) 17–21.
- [42] J. Schiessling, L. Kjeldgaard, F. Rohmund, L. Falk, E. Campbell, J. Nordgren, P.A. Brühwiler, Synchrotron radiation study of the electronic structure of multi-walled carbon nanotubes, *J. Phys. Condens. Matter* 15 (2003) 6563.
- [43] J. Leiro, M. Heinonen, T. Laiho, I. Batirev, Core-level XPS spectra of fullerene, highly oriented pyrolytic graphite, and glassy carbon, *J. Electron Spectrosc. Relat. Phenom.* 128 (2003) 205–213.
- [44] G. Beamson, D. Briggs, *High Resolution XPS of Organic Polymers*, Wiley, 1992.